Original Article

Comparative Analysis of Cyclist Energy Cost and Drag: Able-Bodied vs. Shoulder Amputee Cyclists Using Computational Fluid Dynamics

Short title: Able vs shoulder amputee cyclist energy

Tatiana Sampaio [iD][1,2], Jorge E. Morais [iD][1,2], Daniel A. Marinho [iD][2,3], Tiago M. Barbosa [iD][1,2], António M. Monteiro [iD][1,2], Pedro Forte [iD][1,2,4]

[1] Department of Sports Sciences, Instituto Politécnico de Bragança, Bragança, Portugal
[2] Research Center in Sports Sciences, Health Sciences & Human Development, CIDESD, Covilhã, Portugal
[3] Department of Sports Sciences, University of Beira Interior, Covilhã, Portugal
[4] Instituto Superior de Ciências Educativas do Douro, CI-ISCE, Penafiel, Portugal.

Corresponding author: Departamento de Ciências do Desporto, Escola Superior de Educação, Campus de Santa Apolónia, 5300-253, Bragança, Portugal. **Email:** tatiana_sampaio30@hotmail.com

ABSTRACT

In cycling, drag is the force that opposes the cyclist's motion and is caused by the cyclist's and their equipment's interaction with the air. The surface area of the cyclist and their equipment, such as the bike, helmet, and body postures, substantially impact how much drag they encounter. This study compared the energy cost (Ec) of an able-bodied and shoulder amputee cyclist through numerical simulations using computer fluid dynamics (CFD). According to the hypothesis, an able-bodied cyclist may use more energy at a given speed than an able-bodied cyclist. For this study, a professional male cyclist who weighs 65 kg and is 1.72 m tall took part. The estimated Ec was lower for a shoulder amputee in comparison to an able-bodied cyclist. Significant statistical differences and relationships were found between the cyclists for the 11 selected speeds. Altogether, this study allows us to conclude that, for the same conditions, an able-bodied cyclist delivers less Ec in comparison to a shoulder amputee. Such knowledge contributes to understanding cycling performance and may inform training, equipment design, and energy optimisation strategies for diverse cyclist populations.

Keywords: Energy cost, Drag, Able-Bodied, Amputee.

INTRODUCTION

In cycling, drag is the force that opposes the motion of the cyclist and is caused by the interaction of the cyclist and their equipment with the air (Debraux, Grappe, Manolova, & Bertucci, 2011). The extent of drag that cyclists experience is significantly influenced by the surface area of the rider and their gear, including the bike and helmet (Defraeye, Blocken, Koninckx, Hespel, & Carmeliet, 2011). As expected, an increase in the surface area leads to an augmentation in drag, as well as air resistance due to the heightened exposure of the rider and their gear to the wind (Debraux et al., 2011). In pursuit of optimal aerodynamic performance, cycling equipment manufacturers try to maintain essential functionality while reducing the surface area of the cyclist and their equipment. Adopting a more tucked-in posture has effectively mitigated the surface area exposed to the wind, thus contributing to drag reduction (Forte, Marinho, Barbosa, Morouço, & Morais, 2020). Furthermore, the incorporation of aerodynamic designs, such as teardrop shapes, can impact drag (Forte et al., 2020). To comprehensively evaluate and optimise the cyclist's aerodynamics, a variety of different methods and techniques exist to assess the cyclist's aerodynamics based on experimental testing, numerical simulations, and analytical procedures (mathematical calculations) (Blocken & Toparlar, 2015).

The wind tunnel method is considered the gold standard for assessing aerodynamics (Forte et al., 2015). Still, CFD is less expensive and allows for a wider range of conditions to be simulated. Both CFD and wind tunnel testing have their advantages and limitations. The literature presents that CFD is a valid and precise method to assess cyclists' aerodynamics in comparison to wind tunnel tests (Forte, Morais, Barbosa, & Marinho, 2021). However, it is dependent on the accuracy of the mathematical models used and the quality of the mesh used to discretise the geometry (Yi et al., 2022). Wind tunnel testing provides more accurate

results, but it can be more expensive and may not be able to simulate all the conditions that a cyclist may encounter in the real world (Forte, Barbosa, & Marinho, 2015).

Accordingly, CFD is a simulation approach that examines the movement of fluids, such as air or water, using mathematical formulas and computer modelling (Forte et al., 2015; Blocken, Defraeye, Koninckx, Carmeliet, & Hespel, 2013; Forte et al., 2020; Beaumont, Taiar, Polidori, Trenchard, & Grappe, 2018). The aerodynamics of a bicycle and rider and the impacts of wind resistance, turbulence, and drag may be studied in cycling using CFD (Mannion, Clifford, Blocken, & Hajdukiewicz, 2016). This methodology allows the study of the aerodynamics of amputee cyclists and how the amputations affect their performance in controlled conditions. By modelling the airflow for an able-bodied and amputee cyclist and examining the drag and turbulence created, it will be possible to compare the aerodynamics of cyclists with and without amputation. The outcomes of these simulations may be used to determine whether there are any aerodynamic differences between the two cyclists. CFD may also be used to calculate the energy expenditure of cycling for both able-bodied (Forte, Marinho, Silveira, Barbosa, & Morais, 2020) and amputee cyclists (Forte et al., 2021). This methodology can determine the amount of energy needed to overcome wind resistance and maintain a specific speed. So far, no study has been identified assessing the Ec based on numerical simulations by CFD. Upon that, the aim of this study was to compare the Ec of an able-bodied and shoulder amputee cyclist based on numerical simulations by computer fluid dynamics. It was hypothesised that the able-bodied cyclist may deliver more Ec in comparison to the amputee cyclist for the same speed.

METHODS

Participant

A professional male cyclist who weighs 65 kg and is 1.72 m tall was recruited to participate in this study. The participant was 29 years old and had 15 years of experience at the data collection date. The contestant rides a bicycle with a mass of 7 kg while wearing competition clothing made of polyester, polyamide, polypropylene, and elastane fibres (KTM, Revelator Master 2017). The competitor was taking part in national contests. The Helsinki Declaration was followed at every step of the process, and written informed permission was obtained in advance. The Ethics Committee of the Higher Institute of Educational Sciences of the Douro granted approval.

Scanning

The geometry could be collected while the individual was standing up using a Sense 3D scanner (3D Systems, Inc., Rock Hill, SC, USA) and the appropriate software (Sense, 3D Systems, Inc., Canada) (Blocken, van Druenen, Toparlar, & Andrianne, 2018). The Geomagic Studio software (3D Systems, USA) was used to alter the geometry and convert it to a Computer Aided Design (CAD) model (Barbosa et al., 2017). Then, a new CAD model of a shoulder-amputee cyclist was produced using the same programme. For the able-bodied and shoulder-amputee, editions were to develop bicycle-cyclist system geometries (Figure 1).
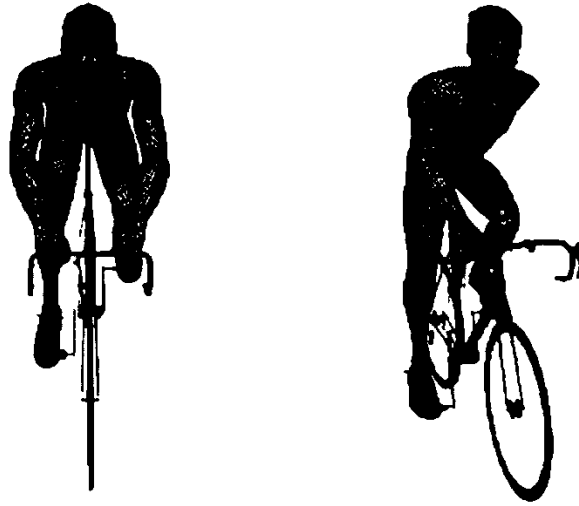
Figure 1. Able-Bodied (left figure) and shoulder-amputee (right figure) bicycle-cyclist geometries, respectively.

Boundary Conditions

In Ansys Workbench software (Ansys Fluent 16.0, Ansys Inc., Pennsylvania, PA, USA), the three-dimensional boundaries surrounding the bicycle-cyclist system were made, measuring 7 metres in length, 2.5 metres in width, and 2.5 meters in height for each configuration. To depict fluid flow in the opposite direction to the bicycle-cyclist systems at a distance of 2.5 m from the fluid flow input part, the Ansys meshing module permitted the generation of a grid with more than 42 million components (Blocken et al., 2013).

The average speed of trips is close to 11.1 m/s (around 40 km/h) (El Helou et al., 2010; Bertucci, Betik, Duc, & Grappe, 2012). Considering that, speeds in increments of 1 m/s up to 13 m/s. At the inlet section of the enclosure surface (-z direction), the velocities were adjusted in the opposite direction from the orientation of the bicycle-cyclist models. In numerical simulations, the turbulence intensity was set to 1×10^6%. Scalable wall functions were given once it was determined that the bicycle-cyclist system had a non-slip wall with zero roughness.

Numerical Simulations

The Reynolds-averaged Navier-Stokes (RANS) equations are solved using the finite volume method by the Fluent CFD algorithm (Ansys Fluent 16.0, Ansys Inc., Pennsylvania, PA, USA). It was decided to use the Realisable k-e turbulence model.

The SIMPLE method was used for the pressure-velocity coupling (Forte, Marinho, Morais, Morouço, & Barbosa, 2018). For the pressure interpolation, convection, and viscous terms, the discretisation techniques were specified as coming in second. The least-squares cell-based approach was used to calculate the gradients. Second-order and second-order upwind were used to determine pressure and momentum, respectively. The first order upwind was used to determine the kinetic energy and dissipation rate of the turbulent flow. Before 1404 contacts, Ansys Fluent 16.0 automatically generated convergence.

Outcomes

Drag Force

The coefficients of drag and effective surface were obtained from the numerical simulations (Ansys Fluent 16.0, Ansys Inc., Pennsylvania, PA, USA). The drag force was computed by Equation (1).

$$F_d = \frac{1}{2}.p.A.Cd.v^2 \tag{1}$$

Fd is the drag force, Cd represents the drag coefficient, v is the velocity, A is the surface area, and ρ is the air density (1.292 kg/m3).

Energy Cost

Knowing drag and rolling resistance, equation (2) enables the assessment of the Ec (i.e., energy expenditure per unit of distance) (Forte, Marinho, Morais, Morouço, & Barbosa, 2018).

$$E_c = \frac{CR.m.g + 0.5.p.A.Cd.v^2}{\eta} \qquad (2)$$

In Equation (2), Ec is the energy cost, CR is the rolling coefficient, m is the body mass of the bicycle-cyclist system, g is the gravitational acceleration, v is the mean velocity over the race, ρ is the air density, A is the surface area, CD the drag coefficient and η the gross efficiency. The assumed gross efficiency of cyclists is 20% (Bertucci et al., 2012) and CR 0.00368 (Forte, Marinho, Morais, Morouço, & Barbosa, 2018).

Statistical Analysis

The normality and homoscedasticity assumptions were analysed using Kolmogorov–Smirnov and Levene tests, respectively. The t-test paired samples compared the two models (able-bodied vs. amputee) as in previous studies (Barbosa, Ramos, Silva, & Marinho, 2018). Cohen's *d* effect size was set as without effect if d < 0.2, moderate effect if 0.8 > d ≥ 0.2, and strong effect if d > 0.5 (Buchheit, 2016).

Simple linear regression models using CFD and analytical procedures were computed for the dataset in SI units. The determination coefficient was computed (R^2). Effect sizes were set as very weak if R^2 < 0.04, weak if 0.04 ≤ R^2 < 0.16, moderate if 0.16 ≤ R^2 < 0.49, high if 0.49 ≤ R^2 < 0.81, and very high if 0.81 ≤ R^2 < 1.0 (Forte et al., 2018; Barbosa et al., 2018).

RESULTS

The Ec varied between 4.13 and 198.60 J/m for the able-bodied and 3.88 and 160.42 J/m for the shoulder amputee. Figure 2 depicts the energy cost of an able-bodied and a shoulder amputee cyclist.
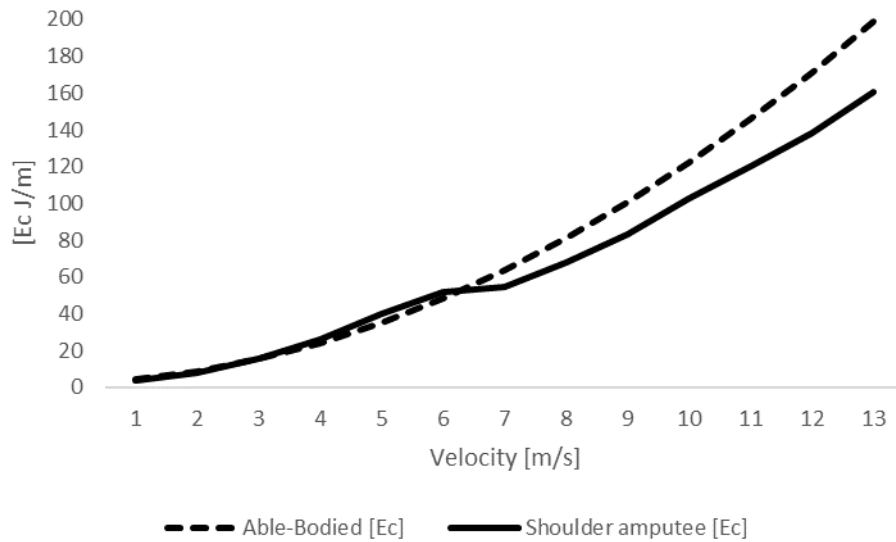

Figure 2. Variations of Ec for able-bodied and shoulder amputee.

The mean Ec at the different velocities was 78.44 (+/- 64.74) J/m for able-bodied and 67.14 (+/- 50.90) J/m for the shoulder amputee cyclist. Statistically significant differences were noted between the able-bodied and shoulder amputee (T = 2.814; p = 0.016; d = 0.78 [0.143 - 1.393]).

The linear regression models produced with able-bodied and shoulder amputee presented a significant relationship and very high effect sizes for Ec in absolute units (R^2 = 0.995; R^2a = 0.997; SEE = 0.02; p < 0.001).

The trend line equation (Y = -6.735 + 1.269x) between methods was above the reference line (Y = x), as presented in Figure 3. Additionally, it was possible to observe that the able-bodied overestimates the shoulder-amputee Ec.
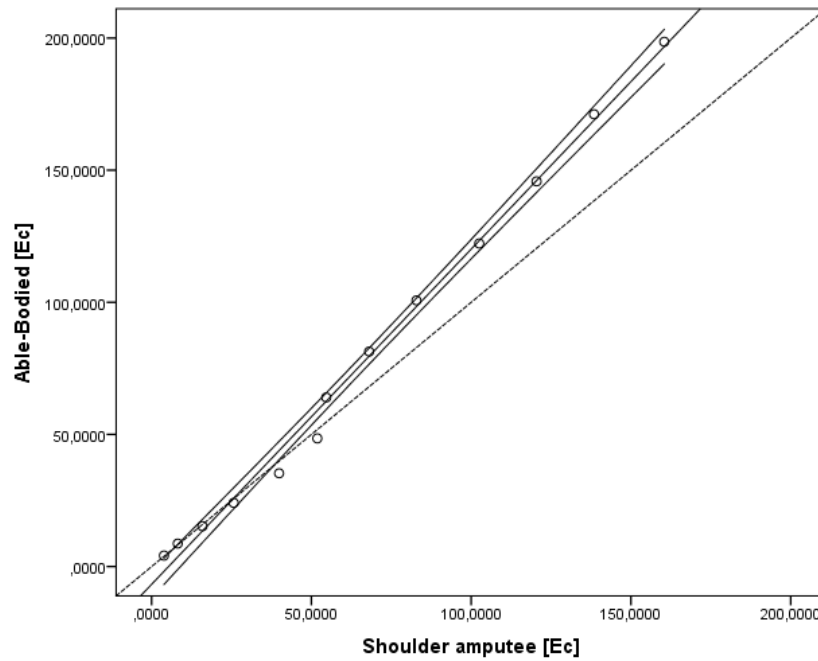
Figure 3. Scattergram, CI lines, tendency line (black) and reference line (dashed black) between able-bodied and shoulder-amputee Ec.

DISCUSSION

The aim of this study was to compare the Ec of an able-bodied and shoulder amputee cyclist based on numerical simulations by computer fluid dynamics. The defined hypothesis was that the able-bodied cyclist may deliver more Ec in comparison to the amputee cyclist for the same speed. The hypothesis was confirmed.

This study was conducted based on numerical simulations to assess the drag and analytical procedures to estimate the rolling resistance (resistive force) and Ec. This methodology has already been used in previous research on cyclists (Forte et al., 2020; Forte et al., 2021).

The Ec exhibited a diverse range, spanning from 4.13 to 198.60 J/m for the able-bodied and 3.88 to 160.42 J/m for the shoulder amputee. Specifically, the mean Ec for the able-bodied amounted to 78.44 (+/- 64.74) J, while the shoulder amputee cyclist demonstrated a mean Ec of 67.14 (+/- 50.90) J. To contextualise these findings, a similar study presents the Ec of a transradial and transtibial cyclist with mean values of 86.17 (± 72.02) J/m and 82.67 (±

67.90) J/m, respectively (Forte et al., 2020). It is worth noting that the presented values for the able-bodied align with the outcomes of a previous study that employed an identical three-dimensional model (Forte et al., 2020). This consistency underscores the reliability and validity of the methodology and further strengthens the comparative analyses across diverse cyclist profiles. The differences may be related to individual characteristics of cyclists and bicycles.

Significant differences were noted for Ec between the able-bodied and the shoulder amputee. The study by Forte et al. (2020) showed no significant differences between transradial and transtibial amputee cyclists in comparison to able-bodied cyclist, which could be explained by the drag differences. The amputee cyclists (transradial and transtibial) drag presented no statistically significant differences in comparison to the able-bodied. It is important to note that the surface area was smaller for amputee cyclists in comparison to the able-bodied cyclist. In these cases, the drag tends to be lower. However, the drag was higher for transradial and transtibial amputees. This could be explained by the possible fluid vorticity around the arm and thigh (Forte et al., 2020). Another study presented the pressure maps of the respective amputees and able-bodied cyclist. It was possible to note that higher pressure was observed in amputee cyclists, resulting in higher drag and Ec (Forte et al., 2021). In the present study, the shoulder amputee presented lower drag in comparison to the able-bodied. We can argue that the vorticity was possibly lower in this case, and the pressure maps had smaller variations, contributing to lower drag (Forte, Morais, Neiva, Barbosa, & Marinho, 2020) in the shoulder amputee. The drag coefficient variations with speed contribute to total drag and Ec variations (Forte et al., 2020).

Additionally, the drag coefficient is susceptible to the object's shape. This has been appointed as an important factor to explain the drag and Ec variations (Forte et al., 2020; Forte et al., 2021). The differences between the able-bodied and shoulder amputees in the present study

are the lack of symmetry and the differences in surface area (lower in the shoulder amputee). Altogether, these factors explain the statistically significant variations in the Ec between the shoulder amputee and the able-bodied cyclist in this study. Such knowledge contributes to understanding cycling performance and may inform training, equipment design, and energy optimisation strategies for diverse cyclist populations.

This study presents the following limitations: (i) only one participant was recruited; (ii) only one position was assessed; (iii) this is a passive (static) analysis; and (iv) only one specific condition was evaluated. However, it is important to highlight that this is the first study comparing the Ec based on CFD and analytical procedures, and the findings of this study showed how much the difference is between the Ec of a shoulder amputee and an able-bodied cyclist.

CONCLUSIONS

The estimated Ec was lower for a shoulder amputee in comparison to an able-bodied cyclist. Significant statistical differences and relationships were found between the cyclists for the 11 selected speeds. Altogether, this study empowers that, for the same conditions, an able-bodied cyclist delivers less Ec compared to a shoulder amputee.

REFERENCES

Barbosa, T. M., Morais, J. E., Forte, P., Neiva, H., Garrido, N. D., & Marinho, D. A. (2017). Correction: A Comparison of Experimental and Analytical Procedures to Measure Passive Drag in Human Swimming. PLoS ONE, 12(5), e0177038.

Barbosa, T. M., Ramos, R., Silva, A. J., & Marinho, D. A. (2018). Assessment of passive drag in swimming by numerical simulation and analytical procedure. Journal of Sports Science, 36(5), 492-498.

Beaumont, F., Taiar, R., Polidori, G., Trenchard, H., & Grappe, F. (2018). Aerodynamic study of time-trial helmets in cycling racing using CFD analysis. Journal of Biomechanics, 67, 1-8.

Bertucci, W. M., Betik, A. C., Duc, S., & Grappe, F. (2012). Gross efficiency and cycling economy are higher in the field as compared with on an Axiom stationary ergometer. Journal of Applied Biomechanics, 28(6), 636-644.

Blocken, B., & Toparlar, Y. (2015). A following car influences cyclist drag: CFD simulations and wind tunnel measurements. Journal of Wind Engineering and Industrial Aerodynamics, 145, 178-186.

Blocken, B., Defraeye, T., Koninckx, E., Carmeliet, J., & Hespel, P. (2013). CFD simulations of the aerodynamic drag of two drafting cyclists. Computers & Fluids, 71, 435-445.

Blocken, B., van Druenen, T., Toparlar, Y., & Andrianne, T. (2018). Aerodynamic analysis of different cyclist hill descent positions. Journal of Wind Engineering and Industrial Aerodynamics, 181, 27-45.

Buchheit, M. (2016). Chasing the 0.2. International Journal of Sports Physiology and Performance, 11(3), 417-418.

Debraux, P., Grappe, F., Manolova, A. V., & Bertucci, W. (2011). Aerodynamic drag in cycling: methods of assessment. Sports Biomechanics, 10(3), 197-218.

Defraeye, T., Blocken, B., Koninckx, E., Hespel, P., & Carmeliet, J. (2011). Computational fluid dynamics analysis of drag and convective heat transfer of individual body segments for different cyclist positions. Journal of biomechanics, 44(9), 1695-1701.

El Helou, N., Berthelot, G., Thibault, V., Tafflet, M., Nassif, H., Campion, F., & Toussaint, J. F. (2010). Tour de France, Giro, Vuelta, and classic European races show a unique progression of road cycling speed in the last 20 years. Journal of Sports Science, 28(8), 789-796.

Forte, P., Barbosa, T. M., & Marinho, D. A. (2015). Technologic appliance and performance concerns in wheelchair racing–helping Paralympic athletes to excel. In C. Liu (Ed.), New Perspectives in Fluid Dynamics (pp. 101-121). Rijeka, Croatia: IntechOpen.

Forte, P., Marinho, D. A., Barbosa, T. M., & Morais, J. E. (2020). Analysis of a normal and aero helmet on an elite cyclist in the dropped position. AIMS Biophysics, 7(1), 54-64.

Forte, P., Marinho, D. A., Barbosa, T. M., Morouço, P., & Morais, J. E. (2020). Estimation of an elite road cyclist performance in different positions based on numerical simulations and analytical procedures. Frontiers in Bioengineering and Biotechnology, 8, 538.

Forte, P., Marinho, D. A., Morais, J. E., Morouço, P. G., & Barbosa, T. M. (2018). The variations on the aerodynamics of a world-ranked wheelchair sprinter in the key-moments of the stroke cycle: A numerical simulation analysis. PloS One, 13(2), e0193658.

Forte, P., Marinho, D. A., Morais, J. E., Morouço, P. G., & Barbosa, T. M. (2018). Estimation of mechanical power and energy cost in elite wheelchair racing by analytical procedures and numerical simulations. Computer Methods in Biomechanics and Biomedical Engineering, 21(6), 585-592.

Forte, P., Marinho, D. A., Nikolaidis, P. T., Knechtle, B., Barbosa, T. M., & Morais, J. E. (2020). Analysis of Cyclist's Drag on the Aero Position Using Numerical Simulations and Analytical Procedures: A Case Study. International Journal of Environmental Research and Public Health, 17(9), 3430.

Forte, P., Marinho, D. A., Silveira, R., Barbosa, T. M., & Morais, J. E. (2020). The aerodynamics and energy cost assessment of an able-bodied cyclist and amputated models by computer fluid dynamics. Medicina, 56(5), 241.

Forte, P., Morais, J. E., Barbosa, T. M., & Marinho, D. A. (2021). Assessment of able-bodied and amputee cyclists' aerodynamics by computational fluid dynamics. Frontiers in Bioengineering and Biotechnology, 9, 163.

Forte, P., Morais, J. E., P. Neiva, H., Barbosa, T. M., & Marinho, D. A. (2020). The drag crisis phenomenon on an elite road cyclist—a preliminary numerical simulations analysis in the aero position at different speeds. International Journal of Environmental Research and Public Health, 17(14), 5003.

Mannion, P, Clifford, E, Blocken, B, Hajdukiewicz, M (2016) Assessing aerodynamic performance in cycling using computational fluid dynamics Civil Engineering Research in Ireland Conference (CERI 2016) Galway, Ireland, 29/08/2016- 30/08/2016.

Yi, W., Bertin, C., Zhou, P., Mao, J., Zhong, S., & Zhang, X. (2022). Aerodynamics of isolated cycling wheels using wind tunnel tests and computational fluid dynamics. Journal of Wind Engineering and Industrial Aerodynamics, 228, 105085.